JOURNAL OF GUIDANCE, CONTROL, AND DYNAMICS
Vol. 42, No. 2, February 2019

Distributed Cooperative Onboard Planning for the Conflict Resolution of Unmanned Aerial Vehicles

Jian Yang,* Dong Yin,† Yifeng Niu,‡ and Lincheng Shen§
National University of Defense Technology, 410073 Changsha, People's Republic of China

DOI: 10.2514/1.G003583

The distributed cooperative onboard conflict resolution problem of unmanned aerial vehicles is studied in this paper. First, the dynamics of unmanned aerial vehicles and the safe separation constraint are studied. The monotonicity feature of the constraint condition is analyzed. The distributed conflict resolution problem is modeled as a distributed constraint optimization problem. Second, the distributed constraint optimization problem is solved in two steps. The feasible solutions are searched first, and the overall costs are minimized thereafter. The distributed stochastic gradient descent method is proposed to search the local near-optimal solutions. The self-improving mechanism is proposed to enhance the utilization efficiency of data exchanged among unmanned aerial vehicles. The "virtue adjustment" theorem is defined to motivate the cooperative coordination between unmanned aerial vehicles. Simulation results show that, compared with existing short-term algorithms, our algorithm could reduce the summation of additional flight distances and impacts on flight plans of unmanned aerial vehicles significantly and coordinate the flights of unmanned aerial vehicles in complex scenarios.

I. Introduction

UNMANNED aerial vehicles (UAVs) have been traditionally used in military operations for decades. With the development of related technologies, UAVs have also been deployed in many civil fields, such as agriculture research and management, disaster search-and-rescue operations, surveillance, sensor coverage for threat detection and cargo delivery, etc. [1,2]. In most of these scenarios, it is desirable to have multiple UAVs cooperatively execute one task as a coalition team. As a result, a large number or swarms of UAVs are anticipated to fly in a crowded local airspace. (This paper regards a group of UAVs as a UAV swarm when their tasks are highly coherent; they could fulfill their tasks efficiently only through collaboration.) Furthermore, UAVs would fly in the same airspace with manned planes when they are integrated into a nonsegregated airspace [3]. Any midair collision between UAVs would result in damage of UAV platforms and fatal threat to the ground [1]. To improve flight safety, an efficient conflict detection and resolution (CDR) mechanism is required [4].

A conflict is an event in which two or more UAVs experience a loss of safe distance. The aim of conflict resolution is to keep safe separation for UAVs in a time interval $[0, \tau]$ while reducing additional cost, where τ is the look-ahead time window. The air traffic management (ATM) for UAVs is still in the exploratory stage. Jenie et al. propose a taxonomy of CDR approaches for operating UAVs in an integrated airspace [5]. Different methods can be adopted to address the CDR problem in different stages. The ATM system would play an important role in managing and coordinating UAVs. Many potential airspace conflicts would be avoided in the "procedural" and "manual" phases. In the third phase, the "cooperative" methods would be applied to dealing with the conflict among UAVs when they are in a close distance. The cooperative methods are classified into two categories (i.e., distributed and centralized cooperative methods [6]). As small and middle-size UAVs are predicted to crowd the airspace, the computational complexity and heavy communication load of the centralized method prohibit them from scaling to large numbers or swarms of UAVs [7]. Furthermore, distributed systems may be more robust and more reliable because they are less sensitive to central failure modes [8]. Therefore, the distributed cooperative methods are more appropriate for the high-density UAVs CDR problem.

The safe separation of UAVs could be achieved by long-term trajectory planning methods (τ is in tens of minutes) and short-term reactive methods (τ is in tens of seconds) [2]. The short-term cooperative onboard planning methods can search deconfliction policies when swarms of UAVs are close to each other [9]. The applications of UAV swarms are typically concerned with fulfilling specific tasks. According to the cooperative CDR method, safe separation and other safety consideration are the basic objectives, whereas reducing additional costs and impacts on other traffics are the higher-order goals [10].

The cooperative conflict resolution method has been studied by many communities. The navigation function method considers both the safe separation and preplanned waypoints of aircraft. Roelofsen et al. propose a navigation function-based method [11]. This method proves able to generate collision-free solutions for high-density UAVs conflicts. However, the collision-free paths often lead to inefficient flight deviations. Panyakeow and Mesbahi propose a method that combines the navigation function and the swirling function, which is efficient to reduce unnecessary deviations of UAVs but would result in regular jitter of UAVs flight paths [12]. Alonso-Mora et al. propose the centralized optimization method and decentralized optimization method according to the velocity obstacle (VO) theory [13]. In their method, the safe separation constraint (SSC) is derived from VO. They mainly focus on the small quadrotor related problems, and the velocities of quadrotors may be changed sharply during the flight, which is impractical and inefficient for fixed-wing UAV swarms. Jenie et al., based on a study on fixed-wing UAVs, propose the selective velocity obstacle (SVO) method [14], which takes the maneuvering regulations under visual flight rules for manned flight into consideration. The SVO could find collision-free solutions to reduce the deviations from nominal flight paths. To guarantee a consensus of the distributed system, each UAV is allocated with fixed responsibility without considering its situation, which often leads to unnecessary detours. Wang et al. propose the distributed collision avoidance method by using the barrier certificates method [10], which performs well in the large-scale swarm conflict scenario. However, as the coordination among UAVs

Received 22 January 2018; revision received 5 July 2018; accepted for publication 11 July 2018; published online 5 October 2018.

*Ph.D. Candidate, College of Intelligence Science and Technology, No. 109, Deya Road, Kaifu District.

†Associate Professor, College of Intelligence Science and Technology, No. 109, Deya Road, Kaifu District.

‡Associate Professor, College of Intelligence Science and Technology, No. 109, Deya Road, Kaifu District; niuyifeng@nudt.edu.cn (Corresponding Author).

§Professor, College of Intelligence Science and Technology, No. 109, Deya Road, Kaifu District.

is assured by predefined rules rather than online information exchange, the algorithm may generate conservative solutions that lead to large detours.

In our previous work, the centralized and distributed cooperative conflict resolution of UAVs is studied in virtue of the geometric methods [6,15,16]. In the centralized method, the stochastic parallel gradient descent method is applied to searching feasible solutions first and then obtaining the local optimal solutions by an efficient optimization solver [6,15]. This method would lead to heavy computation and communication load when the number of UAVs involved in conflicts becomes large. In the distributed method, a linear relationship between pairwise conflict-involved heterogeneous UAVs is established by using the space mapping method. A protocol-based distributed cooperative CDR algorithm is proposed on the basis of the linear relationship [16]. However, this method would also be inefficient when the number of UAVs involved in conflicts becomes large because there is not an online coordination mechanism for the UAVs.

This paper studies the short-term distributed cooperative onboard conflict resolution method for UAVs. We propose to establish an online coordination mechanism for UAVs, which would be applied to dealing with the high-density UAVs conflict resolution problem. It depends on the communication and onboard computation capabilities of UAVs. Along with the development of communication technologies, wireless devices become promising in UAV communication, such as 3/4/5G and Wi-Fi [17–20]. These methods are anticipated to provide a reliable communication network such that UAVs could communicate with their neighbors along bidirectional links [10]. By exploiting the communication resources, UAVs are able to coordinate with their neighbors and achieve cooperative CDR among UAVs. This paper studies the conflict resolution problem of all classes of small- and middle-size UAVs. There are three avenues to avoiding conflict dangers: changing headings and changing the speeds and altitudes [1]. The heading-change-based conflict avoidance method is studied in this paper.

We find that the SSC of pairwise conflicts has some good features. The SSC is monotonic in each period of the slope function $k_{ji}(\varphi_i, \varphi_j)$. Furthermore, the objective function is piecewise convex. To obtain efficient conflict-free solutions, the distributed cooperative conflict resolution problem is modeled as a distributed constraint optimization problem (DCOP), where the constraints are the dynamic constraints of UAVs and requirements for safe separation. The DCOP is solved in two steps. First, find the feasible solutions, and in the second, search the local near-optimal solutions. By exploiting the natural monotonicity of the SSC, the distributed stochastic gradient descent approach (D-SGD) is applied to solving the DCOP. To reduce the communication load, a self-improving mechanism is proposed, with consideration given to the characteristics of gradient direction. Because one UAV could not control the policies of its neighbors in a distributed environment, this paper defines a virtue adjustment theorem that establishes an online coordination mechanism for the UAVs. The local near-optimal solutions are obtained in virtue of the virtue adjustment theorem based coordination mechanism.

The rest of this paper is organized as follows. The problem formulation is given out in Sec. II. In Sec. III, the distributed cooperative conflict resolution method is studied. A report of simulation results is presented in Sec. IV, and conclusions are given in Sec. V.

II. Problem Formulation

Consider $N > 1$ UAVs approaching a confliction region. For UAV A_i, $i \in N$, we assume the following.

1) A_i flies at a constant altitude during task execution.

2) A_i could build up a reliable communication link with its neighboring UAVs, such that they could exchange information on their states and intents.

3) A_i shares the flight information (preferred flight direction, task priority, etc.) with its neighbors.

4) A_i takes cooperative maneuver by coordinating with its neighbors.

5) The planned maneuvering path could be tracked in a certain time threshold within acceptable error range.

This paper uses the graph $G(t) = (V, E(t))$ to express the relationships among UAVs, where $V = \{1, \ldots, n\}$ is the vertex set. Each vertex denotes one UAV [6]. The edge $(i, j) \in E(t)$ denotes the conflict relationship between A_i and A_j at time t. The neighbors of A_i are denoted by the set N_i (i.e., $N_i = \{j \in I | (i, j) \in E\}$ [21]). In the distributed system, A_i only needs to sense and communicate with its neighbors. Because G consists of UAVs that would influence each other in the local airspace, it is a connected graph. As a result of information exchange with neighboring UAVs, the graph G could be updated timely.

A. Unmanned Aerial Vehicle Dynamics and Control Constraints

The conflict resolution problem in midair is highly dynamic. The dynamic constraints of UAVs should be considered. The dynamic characteristics of A_i are described in a Cartesian coordinate system. The region formed by the x and y axes indicates the horizontal plane, and the z axis represents the altitude. Equation (1) defines the position and velocity of A_i in three dimensions:

$$P_i(t) = \begin{bmatrix} x_i(t) \\ y_i(t) \\ z_i(t) \end{bmatrix} v_i(t) = \begin{bmatrix} v_i(t)\cos\gamma_i(t)\cos\phi_i(t) \\ v_i(t)\cos\gamma_i(t)\sin\phi_i(t) \\ v_i(t)\sin\gamma_i(t) \end{bmatrix}^T$$
$$\dot{v}_i(t) = a_i(t), \qquad \dot{\phi}_i(t) = w_i(t), \qquad \dot{\gamma}_i(t) = \mu_i(t)$$
$$0 \le \phi_i(t) < 2\pi, \qquad -\frac{\pi}{2} \le \gamma_i(t) \le \frac{\pi}{2} \tag{1}$$

where the boldface symbol denotes the vector variable; $\phi_i(t)$ is the course angle and denotes the heading of the velocity vector in the horizontal plane; $\gamma_i(t)$ is the pitch angle; $v_i(t)$ denotes the speed; $a_i(t)$ is the acceleration rate; and $w_i(t)$ and $\mu_i(t)$ describe the horizontal angular velocity and the vertical angular velocity at time t, respectively. The state of A_i is characterized by $X_i^t = (P_i(t), \gamma_i(t), \phi_i(t), v_i(t), w_i(t), \mu_i(t))$. The airspace conflict could be resolved by control over $w_i(t)$ and $\mu_i(t)$ [22]. We assume that $v_i(t)$ would keep almost constant when A_i takes heading maneuver. A_i is subject to control constraints:

$$w_i(t) \in [-w_{\max}^i, w_{\max}^i] \mu_i(t) \in [-\mu_{\max}^i, \mu_{\max}^i] \tag{2}$$

We assume that UAVs would not change their altitudes when executing tasks. Therefore, this paper focuses on the CDR problem in the two-dimensional (2-D) planar space. The state of A_i is simplified as $X_i^t = (\boldsymbol{P}_i(t), \phi_i(t), v_i(t), w_i(t))$.

According to the dynamics of UAVs, the heading change is not achieved instantaneously. However, it is impractical to plan precise maneuver trajectories for a large number of UAVs in a distributed environment. The short-term conflict resolution is to design an appropriate turning angle φ_i in the look-ahead time interval $[0, \tau]$. A_i is assumed capable of tracking φ_i within an acceptable error range. The modified path is approximated by Dubins curves as shown in Fig. 1 [16].

The maximum reachable turning angular is obtained by τ and $w_{\max}^i$, which is denoted as $\varphi_{\max}^i(\tau)$. Because τ is tens of seconds in short-term conflict resolution, we define $\varphi_{\max}^i(\tau) \le \pi/3$. φ_i respects the constraint:

$$\varphi_i \in [-\varphi_{\max}^i(\tau), \varphi_{\max}^i(\tau)] \tag{3}$$

The flight path of each UAV is regarded as a straight path in the onboard planning process (see the dot-dashed line in Fig. 1). The Euclidean distance between the initial point and the end point is shorter than the real flight distance in τ. The deviation would be eliminated by the UAV platform in the path tracking process.

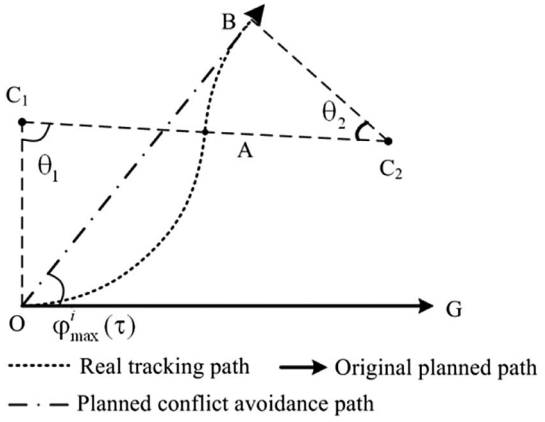

Fig. 1 UAVs track the planned path.

B. Safe Region

The safe region of A_i in a three-dimensional space is a sphere centered at $\boldsymbol{P}_i(t) = (x_i(t), y_i(t), z_i(t))$ with safe radius r_i:

$$D_i(\boldsymbol{P}_i(t), r_i) = \left\{\boldsymbol{P}_s \middle| \|p_s^x - x_i(t), p_s^y - y_i(t), p_s^z - z_i(t)\| < r_i\right\} \quad (4)$$

The range of $D_i(\boldsymbol{P}_i(t), r_i)$ is based on the state and platform (such as size, material, and maneuverability) of A_i. Because the conflicts among UAVs are resolved in the planar 2-D space, the safe region in a 2-D space is defined as $D_i(\boldsymbol{P}_i(t), r_i) = \{\boldsymbol{P}_s | \|p_s^x - x_i(t), p_s^y - y_i(t)\| < r_i\}$. The safe radii of UAVs are set to be hundreds of meters [23].

C. Safe Separation Constraint

The relationship between UAVs is analyzed by local coordinates. As shown in Fig. 2, the position of A_j is set as the original point of the local coordinates frame. The coordinates of A_i at $t = 0$ are

$$\boldsymbol{P}_i(0) = \left(p_i^x(0) - p_j^x(0), p_i^y(0) - p_j^y(0)\right) \quad (5)$$

Assuming that A_i is static, the velocity of A_j relative to A_i is

$$v_{ji}(t) = \left(v_j^x(t) - v_i^x(t), v_j^y(t) - v_i^y(t)\right) \quad (6)$$

$D_{ij}(\boldsymbol{P}_i(0), r_s^{ij})$ is the compound safe region of A_i and A_j, where $r_s^{ij} = \max(r_i, r_j)$. The displacement of A_j relative to A_i in $[0, \tau]$ is denoted as $\boldsymbol{S}_{ji}$. To guarantee safe separation, $\boldsymbol{S}_{ji}$ should be outside $D_{ij}(\boldsymbol{P}_i(0), r_s^{ij})$. This requirement is reduced to two kinds of mathematical constraints, namely, the terminal point constraint and tangential constraint [6]. The tangential constraint prohibits $\boldsymbol{S}_{ji}$ from being the secant line of $D_{ij}(\boldsymbol{P}_i(0), r_s^{ij})$. In the tangential constraint, the conflict-free maneuvers angles φ_i and φ_j are determined by computation once, as shown in Fig. 2b, which is more efficient than the terminal point constraint. To reduce the computational and communication load, the tangential constraint is used as the SSC.

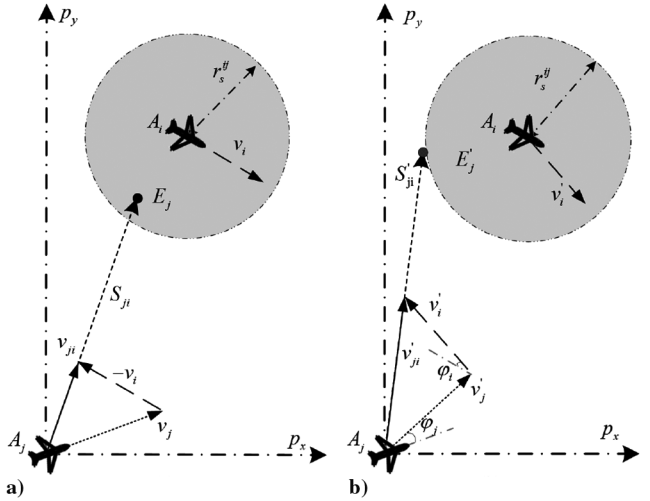

Fig. 2 Representations of a) two UAVs in conflict, and b) cooperative conflict resolution based on the tangential constraint.

The length of the perpendicular segment from $\boldsymbol{P}_i(0)$ to $\boldsymbol{S}_{ji}$ is

$$g(\varphi_i, \varphi_j) = \left\| \boldsymbol{P}_{ij}(0) - \frac{\boldsymbol{P}_{ij}(0) \cdot \boldsymbol{v}_{ji}(t)}{\|\boldsymbol{v}_{ji}(t)\|_2} \right\|_2 \quad (7)$$

The tangential constraint is expressed as

$$g(\varphi_i, \varphi_j) - r_s^{ij} \geq 0 \quad (8)$$

As stated in the former research, k_{ji} is monotonic in each continuous subspace $D_s^{i,j} = \{\varphi_i, \varphi_j | \phi_i + \varphi_i - \phi_j - \varphi_j \neq 2k\pi\}$ [6]. Equation (7) is compounded by $k_{ji}(\varphi_i, \varphi_j)$ and $f_2(x)$, where

$$f_2(x) = |-xP_{ix} + P_{iy}|/\sqrt{1 + x^2} \quad (9)$$

There are one minimum point $x_p^1 = P_{iy}/P_{ix}$ and one maximum point $x_p^2 = -P_{ix}/P_{iy}$ for $f_2(x)$. The interaction angle between $\boldsymbol{S}_{ji}$ and $\boldsymbol{P}_j\boldsymbol{P}_i$ is defined as $\mathcal{A}_{ij}^{vp}$. $g(\varphi_i, \varphi_j)$ reaches the maximum when $k_{ji}(\varphi_i, \varphi_j) = -P_{ix}/P_{iy}$, where $\mathcal{A}_{ij}^{vp} = \pi/2$. $g(\varphi_i, \varphi_j)$ reaches the minimum when $k_{ji}(\varphi_i, \varphi_j) = P_{iy}/P_{ix}$, where $\mathcal{A}_{ij}^{vp} = 0$.

Two UAVs fly away from each other when $\mathcal{A}_{ij}^{vp}$ is an obtuse angle [24]. However, $g(\varphi_i, \varphi_j)$ is smaller than $\|\boldsymbol{P}_i(0)\|$ under this condition, which would lead to misjudgment on the relationship between A_i and A_j, as shown in Fig. 3a [$S^i = (0, 0, \pi/3, 0.05$ km/s), $S^j = (1.5, 1.5, -\pi/3, 0.025$ km/s)]. To correct the judgment, function $g^t(\varphi_i, \varphi_j)$ is defined as Eq. (10):

$$g^i(\varphi_i, \varphi_j) = \begin{cases} g(\varphi_i, \varphi_j) & \text{if } \mathcal{A}_{ij}^{vp} < \pi/2 \\ \|\boldsymbol{P}_i(0)\| & \text{otherwise} \end{cases} \quad (10)$$

Figure 3b shows the shape of $g^t(\varphi_i, \varphi_j)$. There are two monotonic regions for $g^t(\varphi_i, \varphi_j)$, and they are determined by the periods of $k_{ji}(\varphi_i, \varphi_j)$ [6].

One UAV may conflict with two or more other UAVs when many UAVs fly in the local airspace. As a UAV maneuvers to avoid conflicts in a congested airspace, secondary conflicts may follow. Current and potential secondary conflicts must be considered [6]. A variable cr_{ij} is defined as follows:

$$cr_{ij} = \begin{cases} 1 & A_i \text{ current/potential secondary conflict with } A_j \\ 0 & \text{otherwise} \end{cases} \quad (11)$$

D. Objective Function

As discussed in our previous work, the requirement for safe separation and performance limitations are regarded as hard constraints, and other desirable behaviors are expressed in the objective function [16].

The conflict avoidance process is shown in Fig. 4. It may lead to time delay for arrival at the predefined waypoint and deviation from the preferred path. The information exchanged among UAVs could be more sufficient, which is different from the rule-based coordination methods. As different UAVs execute different tasks, the time delays and deviations may have different influences on them. Two coefficients ρ_t^i and ρ_d^i are defined. ρ_t^i and ρ_d^i denote the influences of time delay and deviation from the nominal path on A_i, respectively. The deviation and time delay of A_i incurred by φ_i are discussed in [16].

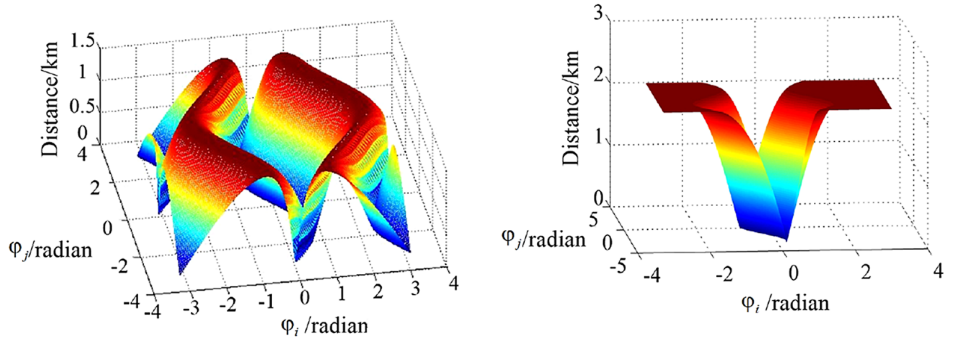

a) b)

Fig. 3 Representations of a) the value of $g(\varphi_i,\varphi_j)$ in range $\varphi_i, \varphi_j \in [-\pi,\pi]$, and b) the value of $g^t(\varphi_i,\varphi_j)$.

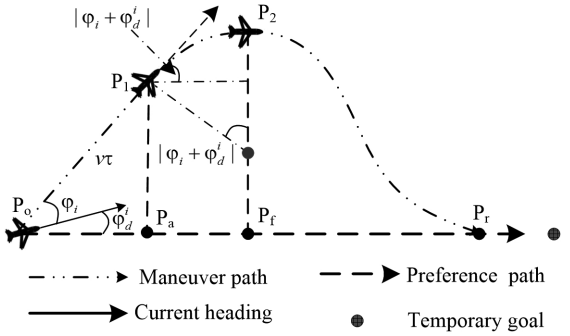

Fig. 4 Conflict avoidance process [16].

The cost of φ_i is a combination of the fuel consumption and influences of time delay on and deviation from the task of A_i:

$$f^i_{\cos t}(\varphi_i) = (\varsigma_i + \rho^i_t)v_i\tau + \Big((\varsigma_i + \rho^i_t)\gamma + \rho^i_d\Big)R^{\text{horizontal}}_{\min,i} + R^{\text{horizontal}}_{\min,i}(\varsigma_i + \rho^i_t)|\varphi_i + \varphi^i_d| + \sqrt{\kappa^{12}_i + \kappa^{22}_i}\sin(|\varphi_i + \varphi^i_d| - \varphi^i_\eta) \tag{12}$$

where ς_i is a coefficient that converts the flight distance into fuel cost, $\kappa^1_i = v_i\tau\gamma(\varsigma_i + \rho^i_t) - R^{\text{horizontal}}_{\min,i}(\varsigma_i + \rho^i_t) + \rho^i_d v_i\tau, \kappa^2_i = v_i\tau(\varsigma_i + \rho^i_t) + \gamma(\varsigma_i + \rho^i_t) + \rho^i_d R^{\text{horizontal}}_{\min,i}$, and $\varphi^i_\eta = \arcsin(\kappa^2_i/\sqrt{\kappa^{12}_i + \kappa^{22}_i})$. γ is a constant coefficient.

There are two variable parts in $f^i_{\cos t}(\varphi_i)$, namely $R^{\text{horizontal}}_{\min,i}(\varsigma_i + \rho^i_t)|\varphi_i + \varphi^i_d|$ and $\sqrt{\kappa^{12}_i + \kappa^{22}_i}\sin(|\varphi_i + \varphi^i_d| - \varphi^i_\eta)$. Both are piecewise monotonic. Therefore, $f^i_{\cos t}(\varphi_i)$ is piecewise monotonic in the maneuverable range.

E. Distributed Cooperative Conflict Resolution Model

The CDR problem is modeled as a local centralized optimization problem in [6]. However, there is not a centralized coordinator in the distributed environment. The aim of A_i is to maximize its utility function U_i in the distributed environment. To facilitate the cooperative coordination among UAVs, U_i should be a function of Φ^i_s, where $\Phi^i_s = \{\varphi_1, \ldots, \varphi_{N_i}\}$ is the set of the maneuver policies of UAVs that conflict with A_i. The objective of distributed cooperative conflict resolution is to search the deconfliction policy Φ_s that could reduce the overall costs in the network. It is modeled as a distributed constraint optimization problem (DCOP). The object of the distributed optimization problem is defined as Eq. (13):

$$\underset{\Phi\in R^N}{\text{Min}}\, U(\Phi_s) = \sum_{i=1}^{N} U_i(\Phi^i_s) \tag{13}$$

such that

$$\phi_i = \phi_i(0), \quad v_i = v_i(0), \quad x_i = x_i(0), \quad y_i = y_i(0)$$
$$g^t_{ij}(\varphi_i,\varphi_j) \geq r^{ij}_s, \quad r^{ij}_s = \max(r_i, r_j) \quad \text{if } cr_{ij} = 1$$
$$-\varphi^i_{\max}(\tau) \geq \varphi_i \geq \varphi^i_{\max}(\tau)i, \qquad j \in N \tag{14}$$

where $\Phi_s = \{\varphi_1, \ldots, \varphi_N\}$ denotes the maneuver policies of UAVs in G.

III. Distributed Cooperative Conflict Detection and Resolution

The ultimate goal of cooperative CDR is to minimize the summation of utilities of UAVs in the network [10]. The problem is solved in two steps; in the first step, find feasible solutions, and in the second, search the local optimal solution from the feasible solutions.

A. Find Feasible Solutions

In the first step, the goal is to find feasible solutions. To facilitate UAVs to take cooperative maneuvers, the utility function of A_i is defined as

$$U_i(\Phi^i_s) = -\frac{1}{2}\sum_{k=1}^{N_i} c_{ik} \tag{15}$$

where c_{ik} is defined as Eq. (16):

$$c_{ik} = \lambda_0(g^t(\varphi_i,\varphi_k)) + (1 - \lambda_0(g^t(\varphi_i,\varphi_k)))g^t(\varphi_i,\varphi_k)/r^{ik}_s \tag{16}$$

$\lambda_0(x)$ is an indicator function. $\lambda_0(x) = 1$ if $x \geq r^{ik}_s$, and $\lambda_0(x) = 0$ if $x < r^{ik}_s$. The maximum of c_{ik} is 1.

$U_i(\Phi^i_s)$ is determined by the spatial relations between A_i and its neighbors. $g^t(\varphi_i,\varphi_k)$ is monotonic in each period of k_{ji}. Therefore, UAVs would take cooperative maneuvers to find conflict-free solutions, aimed at reducing $U_i(\Phi^i_s)$. When all the UAVs obtain conflict-free solutions, the summation of $U_i(\Phi^i_s), i \in N$ would reach the minimum.

1. *Find the Initial Feasible Solution by Distributed Optimization*

Two UAVs would share information with each other when they meet with pairwise conflict. They could obtain conflict-free solutions by applying a gradient descent algorithm because $g^t(\varphi_i,\varphi_k)$ is monotonic in each period of k_{ji}. Assuming that UAVs are synchronized, and the constant sampling period $T > 0$, we denote the UAVs motion variables at time kT by $\Phi^{ij}_k = \Phi(kT) = [\varphi_{i,k}, \varphi_{j,k}]$. Two UAVs start at $\Phi^{ij}_0 = [\varphi_{i,0}, \varphi_{j,0}]$ and update their motion states according to

$$\varphi_{i,k+1} = \varphi_{i,k} - \gamma_k \frac{\partial g^t_{ij}}{\partial \varphi_i}\bigg|\Phi^{ij}_k \tag{17}$$

where γ_k is the chosen coefficient. A_i and A_j could obtain a feasible solution asymptotically by applying the update policy [Eq. (17)].

A_i may conflict with two or more UAVs in the multi-UAV conflict situation. The basic elements of multi-UAV conflict are pairwise conflicts. There would be multiple pairwise gradient directions for A_i because it is involved in multiple pairwise conflicts, such as

$$\left(\frac{\partial g_{ij}^t}{\partial \varphi_i}\middle|\Phi_k^{ij}, \frac{\partial g_{ij}^t}{\partial \varphi_j}\middle|\Phi_k^{ij}\right) \quad \text{and} \quad \left(\frac{\partial g_{il}^t}{\partial \varphi_i}\middle|\Phi_k^{il}, \frac{\partial g_{il}^t}{\partial \varphi_l}\middle|\Phi_k^{il}\right)$$

The deconfliction constraints would be highly coupled. The onboard processing unit is unable to find the analytic solution for gradient direction when it conflicts with multiple UAVs.

There are innumerable ascent directions $(\Delta\varphi_i, \Delta\varphi_j)$ for g_{ij}^t. A_i could easily generate a direction $\Delta\varphi_i$ that can reduce $U_i(\Phi_s^{i,n})$ by using the stochastic search method, where $\Phi_s^{i,n}$ denotes the latest received maneuvers policies of its neighbors. Supposing that A_i obtains an updated motion state $\Phi_s^{i,n} + \delta\varphi_i$, the change of the utility function is

$$\delta U_i = \left(U_i(\Phi_s^{i,n} + \delta\varphi_i) - U_i(\Phi_s^{i,n})\right) \tag{18}$$

where $\delta\varphi_i$ is the stochastic minor modifications on φ_i, and δU_i is the effect of $\delta\varphi_i$ on U_i in position $\Phi_s^{i,n}$. The calculation of Eq. (18) is easy to process. Therefore, it is applied to the onboard processing unit. The stochastic search method is used to estimate the direction of φ_i that makes $U_i(\Phi_s^{i,n})$ descend. Furthermore, as g_{ij}^t is monotonic in each period of k_{ji}, UAVs could find feasible solutions by using the cooperative stochastic search algorithm. Therefore, the D-SGD algorithm is proposed to search the feasible solution Φ_s^{ini} [6].

The D-SGD algorithm is defined as follows. First, A_i generates φ_i^o as the initial maneuver strategy and broadcasts φ_i^o to neighbors. A_i would begin to search Φ_s^{ini} when it receives $\Phi_s^i(o)$. The search process is as follows.

For the mth perturbation of A_i, a random perturbation vector $\delta\varphi_i^{(m)}$ is imposed on $\varphi_i^{(m)}$. $\delta\varphi_i^{(m)}$ is a random variable that obeys the normal distribution $N(0, \sigma_i^2)$, where σ_i^2 is the perturbation amplitude, the value of which depends on

$$\sum_{k=1}^{N_i} c_{ik}/N_i$$

The variation of U_i is

$$\delta U_i^{(m)} = \left(U_i(\Phi_s^{i(m)} + \delta\varphi_i^{(m)}) - U_i(\Phi_s^{i(m)})\right) \tag{19}$$

The $(m+1)$th parameter φ_i is updated based on

$$\varphi_i^{(m+1)} = \varphi_i^{(m)} - \gamma_i^{(m)} \delta U_i^{(m)} \delta\varphi_i^{(m)} \tag{20}$$

where $\gamma_i^{(m)}$ is the system gain position coefficient. The value of $\gamma_i^{(m)}$ is based on the number of iterations. After $\varphi_i^{(m+1)}$ is obtained, A_i would broadcast $\varphi_i^{(m+1)}$ to its neighbors.

A_i would stop changing φ_i if $U_i^{(m)}$ is equal to $-N_i/2$. It means that all the UAVs obtain the feasible solutions when UAVs in the network stop exchanging data. The feasible solution search process is shown in Fig. 5.

As shown in Fig. 5, A_i detects the conflict with other UAVs first. When the conflict relationships between A_i and their neighbors are clear, it begins to search feasible solutions by iterative cooperative stochastic search. The search process contains four operations, the order of which is denoted by numbers in the circles. In the fourth operation, A_i updates the maneuver policy $\varphi_i^{(m+1)}$ by using the calculation defined in Eqs. (19) and (20).

The distributed computation would halt when m equals a preset number and A_i still has not obtained any feasible solution. The algorithm could obtain an initial feasible solution Φ_s^{ini} in a statistical sense if there are feasible solutions in the local solution region.

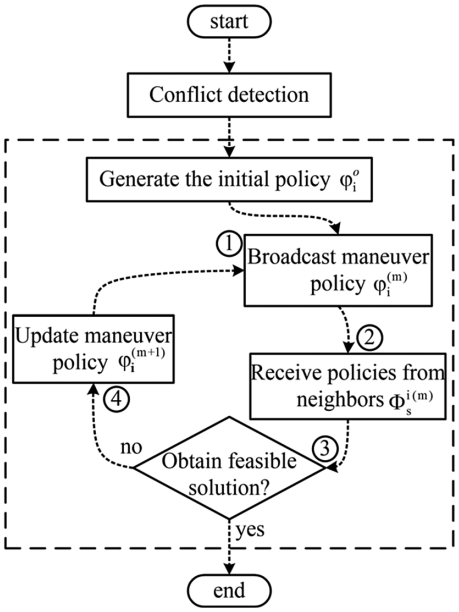

Fig. 5 Feasible solution search process.

2. Self-Improving Mechanism

According to the D-SGD algorithm, UAVs should broadcast the updated maneuver policies to their neighbors in each iteration. The iteration time may be long if UAVs update their maneuver policies merely according to the calculation defined in Eqs. (19) and (20). This would obviously lead to heavy communication load. The communication frequency of the network is often limited in the dynamic environment. UAVs are unable to exchange data with their neighbors at a high frequency. We propose to improve the maneuver policy updating mechanism based on the monotonic feature of $g^t(\varphi_i, \varphi_i)$. According to the multivariable differential calculus, we obtain the following conclusion.

If both $g^t(\varphi_i + \delta\varphi_i, \varphi_j)$ and $g^t(\varphi_i, \varphi_j + \delta\varphi_j)$ are greater than $g^t(\varphi_i, \varphi_j)$, $g^t(\varphi_i + \delta\varphi_i, \varphi_j + \delta\varphi_j)$ would also be greater than $g^t(\varphi_i, \varphi_j)$, which means that $(\delta\varphi_i, \delta\varphi_j)$ is the ascent direction of $g^t(\varphi_i, \varphi_j)$.

According to this feature, the pairwise conflict-involved UAVs are able to improve φ_i and φ_j by searching independently. The self-improving mechanism is proposed to enhance the usage efficiency of exchanged data. It is defined as follows.

In the mth iteration, A_i obtains the updated policies of its neighbors $\Phi_s^{i(m)}$. It would update its maneuver strategy by using the updating rule defined in Eqs. (19) and (20) for a certain number of iterations. The maneuver policies of its neighbors are assumed to be constant and A_i would adjust $\delta\varphi_i^m$ during this calculation process.

After self-improving, UAVs exchange the updated maneuver policies with each other, which is the same as in the original D-SGD algorithm. The time of self-improving iterations should be set to an appropriate value to prevent the computation of each UAV from diverging.

A_i updates $\delta\varphi_i^{(m)}$ to $\delta\varphi_i^{(m+1)}$ in the self-improving phase, as shown in Fig. 6. It then broadcasts $\delta\varphi_i^{(m+1)}$ to its neighbors. The self-improving mechanism would improve the computation efficiency of the onboard device. Therefore, UAVs would obtain feasible solutions

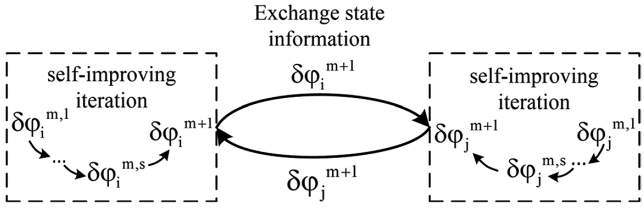

Fig. 6 Self-improving mechanism.

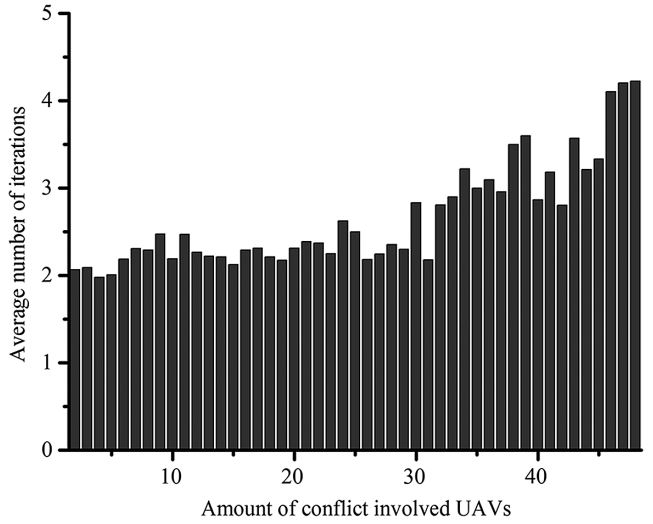

Fig. 7 Average number of interactions of different numbers of UAVs involved in conflicts.

with fewer iterations, which guarantees the algorithm to be applied in infrequent communications networks.

To demonstrate the performance of the self-improving mechanism, a simulation experiment was conducted to study the number of iterations required to obtain feasible solutions for different numbers of UAVs involved in roundabout conflicts. The UAVs were heterogeneous and ranged in number from 2 to 48. The number of iterations in the self-improving process was limited to 15. The average number of interactions between UAVs involved in conflicts is shown in Fig. 7. The results show that UAVs could obtain a feasible solution within no more than five interaction iterations on average. The average number of iterations rose slowly as the number of UAVs involved in a conflict increased. The experiment showed that high-bandwidth communication between UAVs was not required.

B. Search the Local Optimal Solution

The feasible solution of each pairwise conflict is divided into two subregions. In the multi-UAV conflict resolution problem, the global optimal solution would be obtained by searching over 2^{N_c} subregions, where N_c is the number of edges in G. It is impractical to search the global optimal solutions because there is not a centralized coordinator. This paper proposes to search the local optimal solutions by referring to traditional regulation and convention. The rotations of all vehicles to one side often show good results both in centralized and decentralized methods. Therefore, according to this paper, all the conflict-involved UAVs would search from the initial solutions that with the same turning direction.

The initial feasible solution $\Phi_s^{\text{ini}} = \{\varphi_1^{\text{ini}}, \ldots, \varphi_N^{\text{ini}}\}$ may lead to overly large deviations of some UAVs, which would incur unnecessary costs. Because $f^i_{\text{adddis}}(\varphi_i)$ is piecewise monotonic, this paper proposes to improve the solution in the subregion that contains Φ_s^{ini}.

There would be hazards in two folds if A_i only minimizes its own cost function $f^i_{\text{adddis}}(\varphi_i)$. First, the SSC could not be considered comprehensively in the search process. Second, there would be a lack of an efficient mechanism for motivating the cooperative coordination among UAVs. To facilitate the coordination among UAVs, a proper utility function is defined.

The information about the tasks of A_i, such as preference directions, ρ_t^i and ρ_d^i is broadcasted to its neighbors. A_i would consider the maneuver costs of its neighbors if its utility function is defined as in Eq. (21):

$$U_i^* = -\frac{1}{N_i+1}\left(f^i_{\cos t} + \sum_{k=1}^{N_i} f^k_{\cos t}\right) \tag{21}$$

U_i^* implies that the objective of A_i is to minimize the summation of additional cost of its neighbors and itself. Because $f^i_{\cos t}$ is Lipschitz continuity and piecewise monotonic in the local region, the local optimal deconfliction solutions could be obtained by the distributed optimization method.

A_i may incur conflicts with its neighbors if Φ_s^i is modified without considering the safe separation constraint. Therefore, the SSCs are considered as constraints. However, A_i could only modify its own states in the distributed environment. A theorem is designed to build a common knowledge among UAVs, which is able to motivate UAVs to have a tacit mutual understanding without complex communication. UAVs share the belief as defined follows.

When A_i takes a minor adjustment $\delta\varphi_i$ on φ_i, its neighbors would not change their maneuver policies if $\delta\varphi_i$ would not lead to any loss of separation from them, and they would take proper heading adjustments to guarantee the safe separation if $\delta\varphi_i$ leads to a loss of separation from A_i.

According to this belief, named as the virtue adjustment theorem, A_i could devise hypothetical required heading adjustments of its neighbors in self-calculation iterations. Taking the iteration of A_i as an example, supposing that A_i takes a minor random variation $\delta\varphi_i^m$ on φ_i in the mth iteration, its maneuver angle becomes $\varphi_i^{(m)} + \delta\varphi_i^m$. A_i could compute the impact of $\delta\varphi_i^m$ on its space relationships with its neighbors. According to the virtue adjustment theorem, the maneuver policy of A_k is estimated to be $\varphi_k^{(m)} + \delta\varphi_k^{h,i(m)}$, $k \in 1, N_i$ to regain safe separation if A_i and A_k lose separation because of $\delta\varphi_i^m$. The right part above h, i on $\delta\varphi_k^{h,i(m)}$ denotes the estimated modification of A_k by A_i. A_i could obtain the estimated heading deviation vector: $\delta\Phi_s^{h,i(m)} = \{\delta\varphi_i^{(m)}, \delta\varphi_k^{h,i(m)} | k \in N_i\}$ by itself.

To guarantee the convergence of the solution, each UAV makes only minor variation at each time step. We propose to search the local optimal solutions around the feasible solution Φ_s^i by the D-SGD method. First, generate a stochastic minor $\delta\varphi_i^m$. And then, $\delta\Phi_s^{h,i(m)}$ is obtained by A_i. The variation of U_i^* is calculated as Eq. (22):

$$\delta U_i^{*(m)} = \left(U_i^*\left(\Phi_s^{i(m)} + \delta\Phi_s^{h,i(m)}\right) - U_i^*\left(\Phi_s^{i(m)}\right)\right) \tag{22}$$

The parameter updating mechanism is defined as Eq. (23):

$$\varphi_i^{(m+1)} = \varphi_i^{(m)} - \gamma_i^{(m)} \delta U_i^{*(m)} \delta\varphi_i^{(m)} \tag{23}$$

UAVs would broadcast their updated maneuver policies to their neighbors. If $\delta U_i^{*(m)}$ is below a predefined value, A_i would stop changing φ_i. It means that UAVs reach the local near-optimal solutions if there is no data exchange in the network, and the iteration stops. The search iteration would also stop if the search time reaches a predefined value.

Here, we discuss the convergence of the virtue adjustment theorem-based algorithm. It is proved that the SGD algorithm could converge to the local optimal solution in the statistical sense if the variation is small enough. We should prove that the values of elements in $\delta\Phi_s^{h,i(m)}$ are small.

Proof: $g^t(\varphi_i, \varphi_i)$ is continuous in the local space. According to the definition of a continuous function, if $(\delta\varphi_i^{(m)}, 0)$ is in a small range $B_\delta(\varphi_i, \varphi_k)$, the variation of $\delta y = g^t(\varphi_i + \delta\varphi_i^{(m)}, \varphi_k) - g^t(\varphi_i, \varphi_k)$ would also be in a small range $B_\varepsilon(d_o)$. Because $y = g^t(\varphi_i, \varphi_k)$ is monotonic in a small local space, supposing that φ_i is a constant value, the inverse function of g^t for φ_k is defined as

$$\varphi_k = g^{t^{-1}}(y) \tag{24}$$

$g^{t^{-1}}$ is continuous in the local space. According to the feature of a continuous function, because δy is in a small range $B_\varepsilon(y_o)$, the variation of $\delta\varphi_k^{(m)}$ would be in a small range $B_\upsilon(\varphi_k)$.

We could obtain the conclusion that the elements in $\delta\Phi_s^{h,i(m)} = \{\delta\varphi_i^{(m)}, \delta\varphi_k^{h,(m)}, k \in n_i\}$ are guaranteed to be small and that $\Phi_s^{h,i(m)}$

Table 1 Conflict resolution data of eight heterogeneous UAVs

UAV ID	Initial state, km, km, rad, m/s, rad/s	Safe radius, m	Minimum distance, m
A_1	(21, 21, 0.524, 50, 0)	400	537.6
A_2	(23, 21, 1.344, 45, 0)	360	360.5
A_3	(24.5, 21.3, 2.331, 42.5, 0)	340	340.6
A_4	(25.5, 22.5, −3.05, 47.5, 0)	380	380.1
A_5	(25.2, 23.3, −2.44, 52.5, 0)	420	420.2
A_6	(23, 24, −0.629, 37.5, 0)	300	386.1
A_7	(21, 24.3, −0.785, 47.5, 0)	380	420.7
A_8	(22, 22.5, 0, 40, 0)	320	340.6

satisfies the requirement of convergence, depending on the feature of the SGD algorithm.

The modification unit $-\gamma_i^{(m)}\delta U_i^{*(m)}\delta\varphi_i^{(m)}$ is derived based on the random value $\delta\varphi_i^{(m)}$. Furthermore, the minor modifications of Φ_s could not match up without any errors in the distributed environment, and Φ_s may shift out of the feasible region slightly because of $\delta\Phi_s$. The feasible solution search algorithm defined in Sec. III.A is used in the local optimal searching iterations to guarantee Φ_s to return to the feasible region. Because $\delta\Phi_s$ is based on the virtue adjustment theorem and the values are small, Φ_s could be adjusted into the feasible region efficiently by using the feasible solution search method.

C. Discussion on the Communication Environment

As assumed in Sec. II, the distributed cooperation conflict resolution algorithm is based on a reliable communication link among UAVs. UAVs would exchange maneuver policies to update their maneuver policies individually. However, the communication environment may be imperfect in some circumstances. Therefore, we should discuss the performance of this algorithm when the communication environment is imperfect.

In case 1, when the number of handovers is limited, UAVs would be incapable of searching the near-optimal solutions. Because our algorithm is processed in two steps, UAVs could find out feasible solutions with a limited number of handovers.

In case 2, if there is time latency, when one UAV broadcasts its state and maneuver policy, its neighbors would receive its information with time delay. Therefore, UAVs could exchange maneuver policies several seconds one time. In this situation, τ should be set in minutes. The algorithm could find conflict-free solutions only for limited UAVs. The proposed algorithm could not find out conflict-free solution for high-density UAVs conflict. The distributed cooperative algorithm would perform worse than the protocol-based algorithm [16].

IV. Numerical Simulations

The proposed algorithm is tested in numerical simulations. As stated in Sec. II, the speeds of UAVs keep constant while they take heading maneuvers. $w_{\max}^i$ is set to 5 deg/s, the alert distances are set to 3 km, and the safe radii are set to 8^*v_i. The value of τ depends on specific scenarios. Simulations are processed in MATLAB on a dual-core 2.8 GHz Intel i5. The algorithm is executed in each time period. The values of ρ_t^i and ρ_d^i are determined by the tasks and the flight situation of A_i. $\rho_t^{i,o}$ and $\rho_d^{i,o}$ are defined to describe the influence of heading maneuver on the tasks of A_i. $\rho_t^{i,o}$ denotes the influence of time delay. $\rho_d^{i,o}$ denotes the influence of deviation from the nominal path. The values of $\rho_t^{i,o}$ and $\rho_d^{i,o}$ are set as 1, $\forall\, i \in N$. t_d^i is the time delay of A_i compared with the original plan. d_{dev}^i is the distance of deviation from the nominal path [6]. The values of ρ_t^i and ρ_d^i are updated as

$$\rho_t^i = \rho_t^{i,o} + t_d^i/20, \qquad \rho_d^i = \rho_d^{i,o} + d_{\text{dev}}^i \tag{25}$$

where the units of t_d^i and d_{dev}^i are seconds and kilometers, respectively.

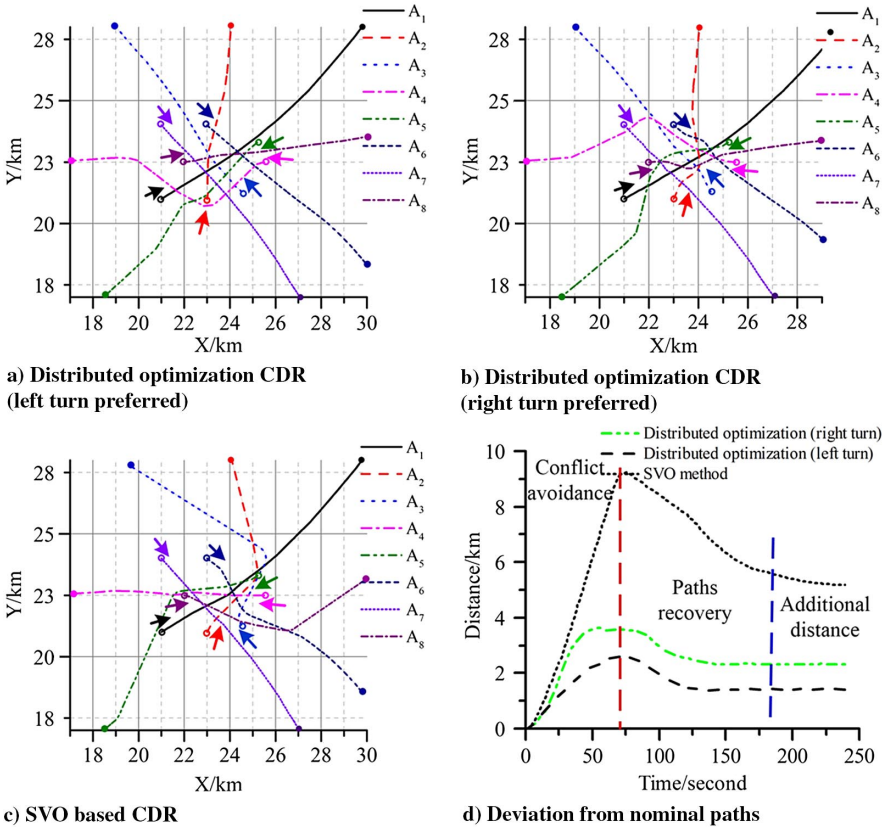

a) Distributed optimization CDR (left turn preferred)

b) Distributed optimization CDR (right turn preferred)

c) SVO based CDR

d) Deviation from nominal paths

Fig. 8 Comparison of multi-UAV conflict resolution results.

Table 2 Performance of two algorithms

Algorithms	d_s, km	t_r, s
Distributed optimization (left turn)	1.42	128
Distributed optimization (right turn)	2.32	144
SVO-based method	5.19	228

A. Algorithms Comparison

Our method is compared with SVO in the first example [14]. Eight heterogeneous UAVs are in the local airspace. The initial states of UAVs are shown in Table 1.

Because the maneuver space of UAVs is limited when UAVs are close to each other. The SVO algorithm requires UAVs to take large detours in some occasions, and it is unable to generate any feasible solution in a crowded environment when τ is small. Therefore, τ is set to be 35 s in this scenario. We define variables d_s and t_r as metrics of the performances of algorithms. d_s records the summation of deviations of the current states from the nominal paths of UAVs. t_r denotes the time that UAVs take to recover from conflict resolution. To demonstrate that the performances are similar when UAVs take a left or right turn, this paper shows that deconfliction is achieved when all the UAVs take a left turn or a right turn. The conflict resolution results are shown in Fig. 8. Table 1 shows the minimum distance between UAVs and their neighbors in the right turn preferred CDR scenario. It demonstrates that these UAVs could keep safe separation by using our algorithm.

The SVO algorithm is able to generate conflict-free solutions without serious impact on the flight paths of UAVs. "Serious" indicates inefficient solutions, which would cause some UAVs to fly around the conflict region until other UAVs fly away [16,25]. Our algorithm outperforms the SVO algorithm because UAVs need only to take minor adjustment. Some UAVs, such as A_1, A_3, and A_6, would fly almost along their nominal paths during the conflict resolution process.

The curves of d_s in conflict resolution scenarios (see Figs. 8a–8c) are shown in Fig. 8d. The conflict resolution is divided into two phases. In the first phase, UAVs take heading maneuvers to avoid conflicts. Therefore, they would depart from the nominal paths. In the second phase, they return to the nominal paths after conflicts are resolved. These curves become flat when UAVs return to the nominal paths. However, because there are distances from the current states to the nominal plans after conflict resolution, the values of these curves are not 0. The values of d_s imply the additional flight distances. Table 2 shows the values of d_s and t_r by using different methods in eight UAVs scenarios. The left/right turn preferred distributed optimization method outperforms the SVO method. Our method would incur smaller additional flight distances, and UAVs would return to the nominal paths rapidly after conflicts are resolved.

B. Simulation of Multi-Unmanned-Aerial-Vehicle Roundabout Scenarios

The multi-agent roundabout scenarios are processed to validate the performance of the proposed algorithms in [7,26]. UAVs are permitted to make speed changes sharply in [7], so that they could even hover in middle air and go through the crowded region by slow adjustment. In [26], agents move at the same speed. Our algorithm is demonstrated in dealing with the conflict of 48 homogeneous UAVs. The speeds of UAVs are 50 m/s. The safe radii of UAVs are 400 m. They are placed evenly in a circle at first and predicted to converge at the position (20, 20 km). With consideration given to the turn rate constraints, crowded environment, and converge conflicts, the value of τ is set to be 40 s. UAVs choose to turn left, and the potential conflicts among UAVs are avoided genteelly. Figures 9a–9c show the conflict-free flight paths of UAVs, which indicate that UAVs would take almost the same maneuvers to keep safe separation. Therefore, the relative space relationships of each UAV to other UAVs are the same. Figure 9d illustrates the curves of minimum distances of UAVs to their neighbors during the flights. The minimum distance curves of all the UAVs are the same. Figure 9d depicts that UAVs could keep

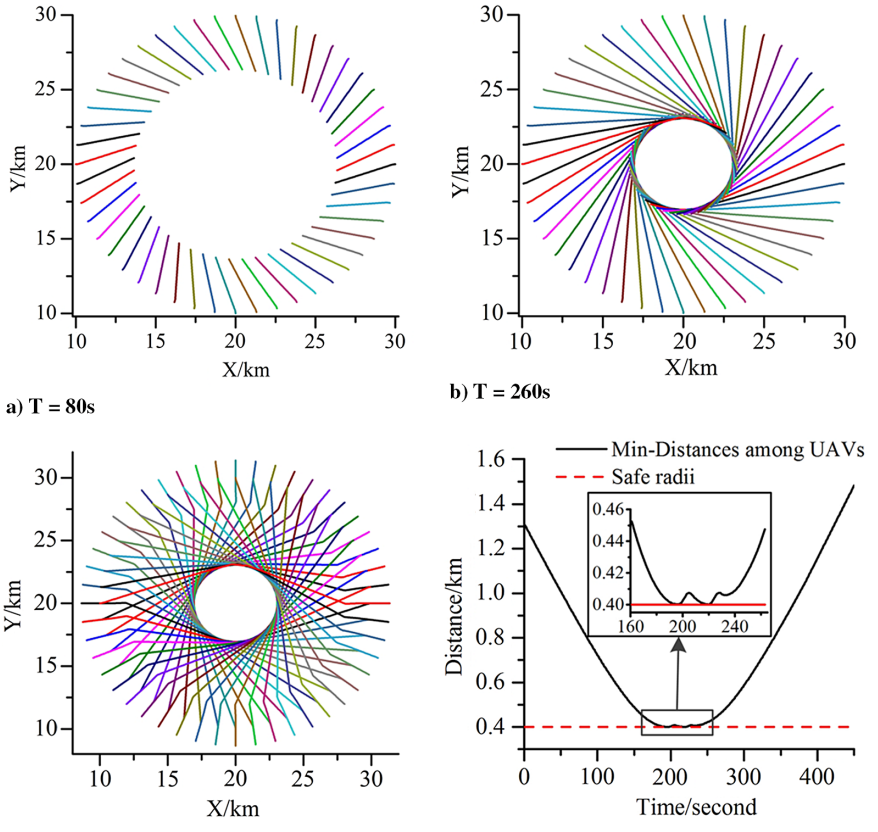

a) T = 80s

b) T = 260s

c) T = 450s

d) Min-distance among UAVs during conflict resolution

Fig. 9 Conflict resolution results of 48 homogeneous UAVs.

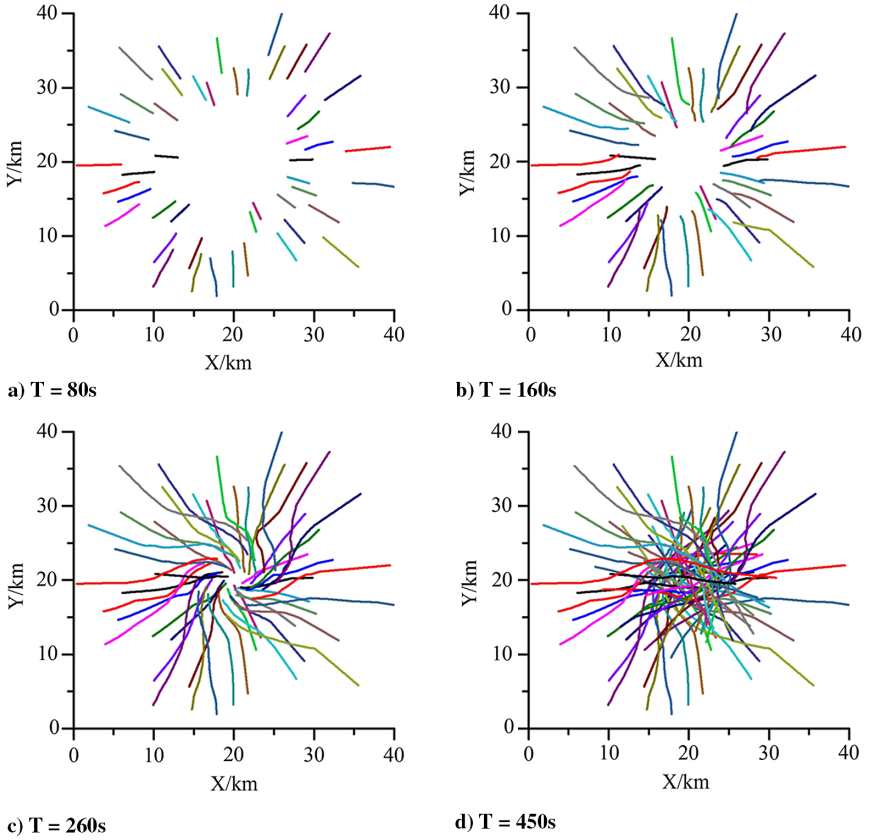

Fig. 10 Conflict-free flight paths of 48 heterogeneous UAVs.

safe separation from others. The black block in Fig. 9d depicts the minimum distances of UAVs when they are close to the conflict region around the position (20, 20 km). It shows that all the UAVs would take minor heading maneuvers to keep the minimum safe separation from others during this process. Therefore, the perimeter of the center white round region is close to 19.2 km, which is equal to $48 \cdot 0.4$ km. Furthermore, UAVs would return to the nominal paths immediately after they pass through the congested region. Therefore, it can be concluded that all the UAVs can obtain good conflict-free solutions.

The roundabout conflicts of homogeneous UAVs are relatively easier than those of heterogeneous UAVs because SSCs are linear when the speeds of UAVs are equal [27]. In the third experiment, the speeds of UAVs are in the range [30, 75 m/s]. In this complex scenario, τ is set to be 50 s. The conflict scenario is resolved by applying the proposed distributed optimization algorithm. The conflict-free flight paths are shown in Fig. 10. UAVs are able to go through the congested region without flying around the congested region.

In the initial feasible solution search process, all the UAVs would be set to initial turn-left maneuver policies. However, some UAVs would find turn-right policies to avoid their neighbors at first. The right-turning UAVs would be affected by the heading directions of their neighbors as time goes on. More and more UAVs take left turns as UAVs converge to the center region. Figure 11a indicates that the number of left-turning UAVs would increase to the maximum value when UAVs are close to the center conflict region, and then the number of left-turning UAVs would decrease sharply when UAVs pass through the conflict region. As a result, the conflict avoidance phase and the paths recovery phase could be explicitly identified according to the number of left-turning UAVs. The conflict resolution results demonstrate that UAVs could generate efficient solutions by turning to the same directions. Therefore, UAVs turning to the same direction is a simple but efficient maneuver strategy in the roundabout scenario.

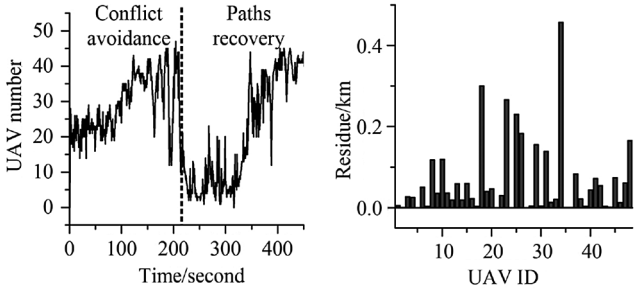

Fig. 11 Representations of a) the number of left turning UAVs during the simulation, and b) residue values of $d^i_{\min} - r_i$.

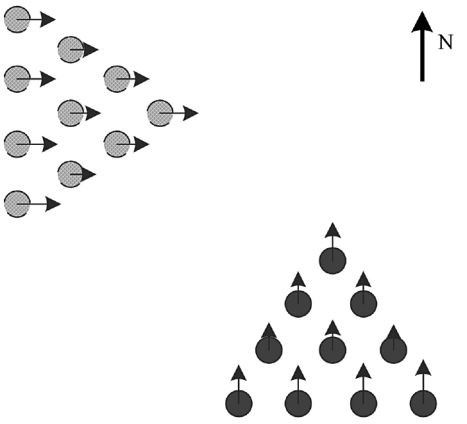

Fig. 12 Conflict scenario involving two groups of UAVs.

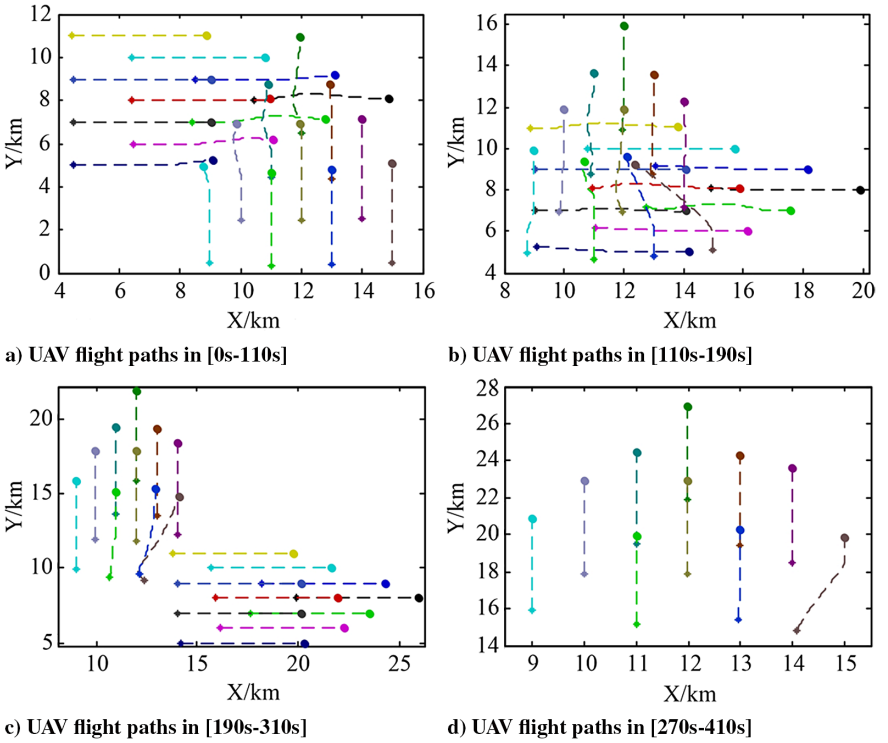

Fig. 13 Conflict resolution result of two groups of UAVs.

Figure 11b shows the residue values of $d^i_{\min} - r_i$, where $d^i_{\min}$ is the minimum distance between A_i and its neighbors during the flight. All values in Fig. 11b are above 0, which demonstrates that UAVs could keep safe separation from their neighbors. Furthermore, Fig. 11b shows that the residue values are close to 0, which means UAVs would not take large heading maneuvers to keep large distances from their neighbors. On the contrary, they would just take moderate maneuvers to keep the minimum safe distances from each other. The ultimate objective of these UAVs is to reduce the additional flight distances.

C. Conflict Resolution in Complex Scenarios

In this section, we will demonstrate some complex conflict resolution scenarios. In the fourth experiment, 20 heterogeneous UAVs are divided into two groups. The speeds of UAVs are in the range [48, 52 m/s]. As shown in Fig. 12, UAVs make up two delta formations. According to the nominal plan, the first group flies from west to east, and the second flies from south to north.

They would meet with conflicts during the flight. UAVs search the local optimal solutions by turning left. τ is set to be 20 s. The flight paths of UAVs are divided into four phases, as shown in Figs. 13a–13d, respectively. The stars and dots denote the initial and terminal positions of UAVs in each phase, respectively. Figure 13d shows the path recovery process of the second group of UAVs.

Table 3 Minimum distances of UAVs in the two group scenarios

UAV ID	Safe radius, m	Minimum distance, m	UAV ID	Safe radius, m	Minimum distance, m
A_1	400	401.6	A_{11}	400	401.6
A_2	408	408.3	A_{12}	392	393.7
A_3	392	393.7	A_{13}	388	408.3
A_4	392	412.9	A_{14}	412	412.9
A_5	400	401.8	A_{15}	400	401.8
A_6	408	408.3	A_{16}	400	408.3
A_7	396	396.4	A_{17}	408	408.5
A_8	404	446.2	A_{18}	392	408.5
A_9	404	404.2	A_{19}	384	404.2
A_{10}	408	409.4	A_{20}	400	409.4

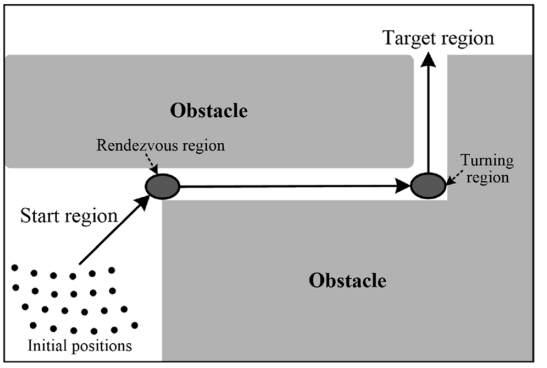

Fig. 14 Flight plan of 24 heterogeneous UAVs.

Two groups of UAVs converge in the congested region. They adjust their headings slightly and return to their nominal paths rapidly. UAVs would not deviate from their nominal paths excessively, which can reduce the impacts on their neighbors. The minimum distances of UAVs from their neighbors are recorded in Table 3. UAVs keep safe separation by using the proposed algorithm.

In the fifth experiment, our algorithm is demonstrated in the presence of obstacles. There are 24 UAVs in the scenario. The initial positions of UAVs are denoted by black spots in Fig. 14. The speeds of UAVs are in the range [48, 52 m/s]. The initial minimum distance between UAVs is 580 m. There are obstacles along the path. The obstacles construct a complex space environment. UAVs should go through the long and narrow region to the target region. The black arrows in Fig. 14 indicate the preplanned paths. The preplanned paths would incur loss of separation among UAVs, especially in the two dark ellipse regions. This scenario demonstrates the capability of our algorithm for dealing with complex conflicts. As UAVs are heading to the same region at almost the same speed, the potential conflict among UAVs should be resolved by moderate heading adjustments. The value of τ is set to be 20 s. Figure 15 shows the conflict-free results by using the proposed algorithm. The flight process is divided into four phases. As shown in Figs. 15a–15d, UAVs would take minor heading changes to keep safe separation during the flight.

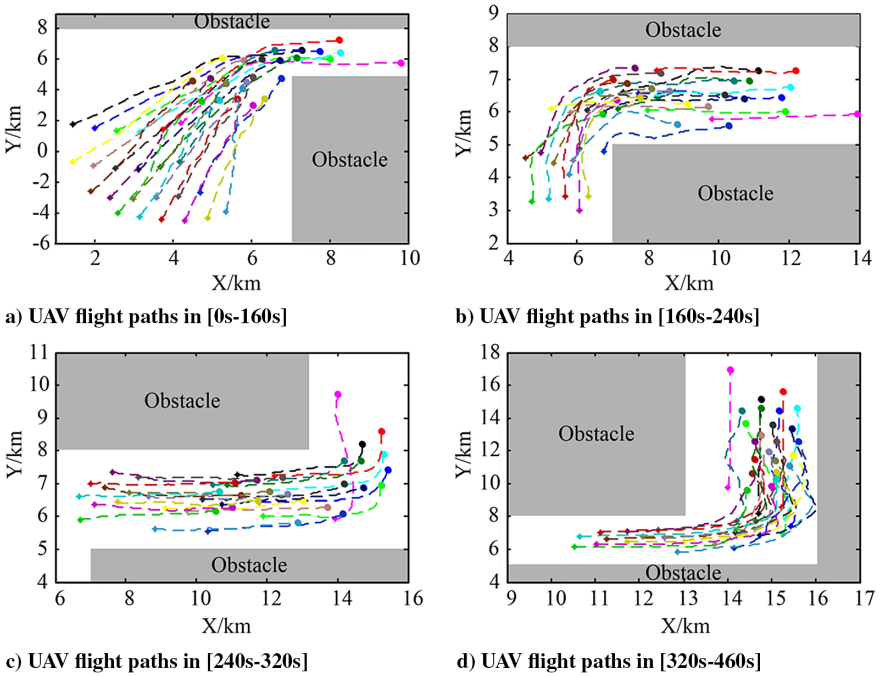

Fig. 15 Conflict resolution results of 24 UAVs.

Table 4 Minimum distances of UAVs in the obstacle environment

UAV ID	Safe radius, m	Minimum distance, m	UAV ID	Safe radius, m	Minimum distance, m
A_1	400	401.2	A_{13}	388	400.3
A_2	408	408	A_{14}	412	424
A_3	392	396.2	A_{15}	400	400.4
A_4	384	396.2	A_{16}	400	400.4
A_5	400	416.6	A_{17}	408	408.1
A_6	412	416.6	A_{18}	392	439.6
A_7	396	404.4	A_{19}	384	409.2
A_8	400	412.4	A_{20}	400	400.3
A_9	408	408.2	A_{21}	412	413.5
A_{10}	408	411.7	A_{22}	392	433.2
A_{11}	400	401.2	A_{23}	400	406.7
A_{12}	392	402.1	A_{24}	408	410.6

The minimum distances between each UAV and their neighbors are recorded in Table 4. It shows that UAVs would keep safe separation during the flight.

V. Conclusions

In this paper, we have presented a distributed constraint optimization model to deal with the distributed cooperative onboard conflict resolution problem for unmanned aerial vehicles (UAVs). The dynamics of UAVs are discussed according to the conflict resolution requirement. The safe separation constraint (SSC) is analyzed based on the geometric method. By comprehensively considering the objective of conflict resolution and the features of the SSCs, the problem is modeled as a distributed constraint optimization problem (DCOP). The distributed stochastic gradient descent algorithm (D-SGD) is proposed to solve the problem. A two-step computation mechanism is designed to find the local near-optimal deconfliction solutions. The self-improving mechanism is applied to enhancing the utilization efficiency of data exchanged among UAVs. This method could greatly reduce the required communication frequency of the network. An online coordination mechanism, which is based on the virtue adjustment theorem, is proposed to motivate the cooperative coordination among UAVs.

The proposed algorithm is implemented and tested in simulations. The simulation system is developed in MATLAB. The proposed algorithm is compared with existing methods. Simulation results demonstrate the satisfactory performance of the proposed algorithm in dealing with complex conflict scenarios.

Acknowledgments

This work was supported in part by the Natural Science Foundation of China (number 61603406, 61876187), the China Postdoctoral Science Foundation (number 2014M552687), and the Graduate Student Innovation Project of Hunan province (number CX2014B013).

References

[1] Dalamagkidis, K., Valavanis, K. P., and Piegl, L. A., "On Unmanned Aircraft Systems Issues, Challenges and Operational Restrictions Preventing Integration into the National Airspace System," *Progress in Aerospace Sciences*, Vol. 44, Nos. 7–8, 2008, pp. 503–519. doi:10.1016/j.paerosci.2008.08.001

[2] Yu, X., and Zhang, Y., "Sense and Avoid Technologies with Applications to Unmanned Aircraft Systems: Review and Prospects," *Progress in Aerospace Sciences*, Vol. 74, April 2015, pp. 152–166. doi:10.1016/j.paerosci.2015.01.001

[3] Sahawneh, L. R., and Beard, R. W., "A Probabilistic Framework for Unmanned Aircraft Systems Collision Detection and Risk Estimation," *Proceedings of the IEEE Conference on Decision and Control*, IEEE Publ., Piscataway, NJ, 2014, pp. 242–247. doi:10.1109/CDC.2014.7039388

[4] Zhou, Y., and Baras, J. S., "Reachable Set Approach to Collision Avoidance for UAVs," *Proceedings of the IEEE Conference on Decision and Control*, IEEE Publ., Piscataway, NJ, 2015, pp. 5947–5952. doi:10.1109/CDC.2015.7403154

[5] Jenie, Y. I., Kampen, E. V., Ellerbroek, J., and Hoekstra, J. M., "Taxonomy of Conflict Detection and Resolution Approaches for Unmanned Aerial Vehicle in an Integrated Airspace," *IEEE Transactions on Intelligent Transportation System*, Vol. 18, No. 3, 2017, pp. 558–567. doi:10.1109/TITS.2016.2580219

[6] Yang, J., Yin, D., Cheng, Q., and Shen, L., "Two–Layered Mechanism of Online Unmanned Aerial Vehicles Conflict Detection and Resolution," *IEEE Transactions on Intelligent Transportation Systems*, IEEE Publ., Piscataway, NJ, Dec. 2017, pp. 1–15. doi:10.1109/TITS.2017.2771465

[7] Hoffmann, G. M., and Tomlin, C. J., "Decentralized Cooperative Collision Avoidance for Acceleration Constrained Vehicles," *Proceedings of the IEEE Conference on Decision and Control*, IEEE Publ., Piscataway, NJ, 2008, pp. 4357–4363. doi:10.1109/CDC.2008.4739434

[8] Pritchett, A. R., and Genton, A., "Negotiated Decentralized Aircraft Conflict Resolution," *IEEE Transactions on Intelligent Transportation System*, Vol. 19, No. 1, 2018, pp. 81–91. doi:10.1109/TITS.2017.2693820

[9] Ong, H. Y., and Kochenderfer, M. J., "Short-Term Conflict Resolution for Unmanned Aircraft Traffic Management," *Proceedings of the IEEE/AIAA Digital Avionics Systems Conference*, IEEE Publ., Piscataway, NJ, 2015, pp. 5A4-1–5A4-13. doi:10.1109/DASC.2015.7311424

[10] Wang, L., Ames, A. D., and Egerstedt, M., "Safety Barrier Certificates for Collisions-Free Multirobot Systems," *IEEE Transactions on Robotics*, Vol. 33, No. 3, 2017, pp. 661–674. doi:10.1109/TRO.2017.2659727

[11] Roelofsen, S., Martinoli, A., and Gillet, D., "Distributed Deconfliction Algorithm for Unmanned Aerial Vehicles with Limited Range and Field of View Sensors," *Proceedings of the 2015 American Control Conference*, IEEE Publ., Piscataway, NJ, 2015, pp. 4356–4361. doi:10.1109/ACC.2015.7172014

[12] Panyakeow, P., and Mesbahi, M., "Deconfliction Algorithms for a Pair of Constant Speed Unmanned Aerial Vehicles," *IEEE Transactions on Aerospace and Electronic Systems*, Vol. 50, No. 1, 2014, pp. 456–476. doi:10.1109/TAES.2013.110766

[13] Alonso-Mora, J., Naegeli, T., Siegwart, R., and Beardsley, P., "Collision Avoidance for Aerial Vehicles in Multi-Agent Scenarios," *Autonomous Robots*, Vol. 39, No. 1, 2015, pp. 101–121. doi:10.1007/s10514-015-9429-0

[14] Jenie, Y. I., Kampen, E. V., Visser, C. C. D., Ellerbroek, J., and Hoekstra, J. M., "Selective Velocity Obstacle Method for Deconflicting Maneuvers Applied to Unmanned Aerial Vehicles," *Journal of Guidance, Control, and Dynamics*, Vol. 38, No. 6, 2015, pp. 1140–1145. doi:10.2514/1.G000737

[15] Yang, J., Yin, D., Shen, L., Cheng, Q., and Xie, X., "Cooperative Deconflicting Heading Maneuvers Applied to Unmanned Aerial Vehicles in Non-Segregated Airspace," *Journal of Intelligent & Robotic Systems*, Vol. 92, No. 1, Sept. 2018, pp. 187–201. doi:10.1007/s10846-017-0766-4

[16] Yang, J., Yin, D., and Shen, L., "Reciprocal Geometric Conflict Resolution on Unmanned Aerial Vehicles by Heading Control," *Journal of Guidance, Control, and Dynamics*, Vol. 40, No. 10, 2017, pp. 2511–2523. doi:10.2514/1.G002607

[17] Asadpour, M., Van den Bergh, B., Giustiniano, D., Hummel, K. A., Pollin, S., and Plattner, B., "Micro Aerial Vehicle Networks: An Experimental Analysis of Challenges and Opportunities," *IEEE Communications Magazine*, Vol. 52, No. 7, 2014, pp. 141–149. doi:10.1109/MCOM.2014.6852096

[18] Andre, T., Hummel, K. A., Schoellig, A. P., Yanmaz, E., Asadpour, M., Bettstetter, C., Grippa, P., Hellwagner, H., Sand, S., and Zhang, S., "Application-Driven Design of Aerial Communication Networks," *IEEE Communications Magazine*, Vol. 52, No. 8, 2014, pp. 129–137. doi:10.1109/MCOM.2014.6815903

[19] Oubbati, O. S., Lakas, A., Zhou, F., Günes, M., and Yagoubia, M. B., "A Survey on Position-Based Routing Protocols for Flying Adhoc Networks (FANETs)," *Vehicular Communications*, Vol. 10, Oct. 2017, pp. 29–56. doi:10.1016/j.vehcom.2017.10.003

[20] Verstraeten, J., Stuip, M., and Birgelen, T. V., "Assessment of Detect and Avoid Solutions for Use of Unmanned Aircraft Systems in Nonsegregated Airspace," *Handbook of Unmanned Aerial Vehicles*, Springer, Dordrecht, The Netherlands, 2014, pp. 1955–1979. doi:10.1007/978-90-481-9707-1_70

[21] Yang, J., Yin, D., Cheng, Q., and Xie, X., "Two-Layer Optimisation to Cooperative Conflict Detection and Resolution for UAVs," *Proceedings of the 18th International Conference on Intelligent Transportation System*, IEEE Publ., Piscataway, NJ, 2015, pp. 2072–2077. doi:10.1109/ITSC.2015.335

[22] Jenie, Y. I., Kampen, E. V., Visser, C. C. D., Ellerbroek, J., and Hoekstra, J. M., "Three-Dimensional Velocity Obstacle Method for Uncoordinated Avoidance Maneuvers of Unmanned Aerial Vehicles," *Journal of Guidance, Control, and Dynamics*, Vol. 39, No. 10, 2016, pp. 2312–2323. doi:10.2514/1.G001715

[23] Jamoom, M. B., Joerger, M., and Pervan, B., "Unmanned Aircraft System Sense-and-Avoid Integrity and Continuity Risk," *Journal of Guidance, Control, and Dynamics.*, Vol. 39, No. 3, 2016, pp. 498–509. doi:10.2514/1.G001468

[24] Vela, A., Feigh, K. M., Solak, S., Singhose, W., and Clarke, J., "Formulation of Reduced-Taskload Optimization Models for Conflict Resolution," *IEEE Transactions on Systems, Man and Cybernetics, Part A: Systems and Humans*, Vol. 42, No. 6, 2012, pp. 1552–1561. doi:10.1109/TSMCA.2012.2202106

[25] Roelofsen, S., Martinoli, A., and Gillet, D., "Distributed Deconfliction Algorithm for Unmanned Aerial Vehicles with Limited Range and Field of View Sensors," *Proceedings of the 2015 American Control Conference*, IEEE Publ., Piscataway, NJ, 2015, pp. 4356–4361. doi:10.1109/ACC.2015.7172014

[26] Lalish, E., and Morgansen, K. A., "Distributed Reactive Collision Avoidance," *Autonomous Robots*, Vol. 32, No. 3, 2012, pp. 207–226. doi:10.1007/s10514-011-9267-7

[27] Pallottino, L., Feron, E. M., and Bicchi, A., "Conflict Resolution Problems for Air Traffic Management Systems Solved with Mixed Integer Programming," *IEEE Transactions on Intelligent Transportation System*, Vol. 3, No. 1, 2002, pp. 3–11. doi:10.1109/6979.994791